Origin of Tourmaline in the Setters Formation, Maryland:
Evidence from Major and Trace Element, Boron Isotope, and Rare Earth Element Characteristics

Joseph F. Browning
Advisors: Philip M. Piccoli and Richard D. Ash
Department of Geology, University of Maryland at College Park

I. Background

The Setters Formation is a 0-750 ft thick, Cambro-Ordovician, metasedimentary unit that comprises interbedded massive quartzite and schist. Because the Setters breaks easily along the schist foliation plane to form flagstone slabs, the rock has been historically quarried for construction material.

The Setters Formation is found outcropping to the north and west of Baltimore, MD. Sample collection for this research project focused on the Woodstock Dome, located west of Baltimore.

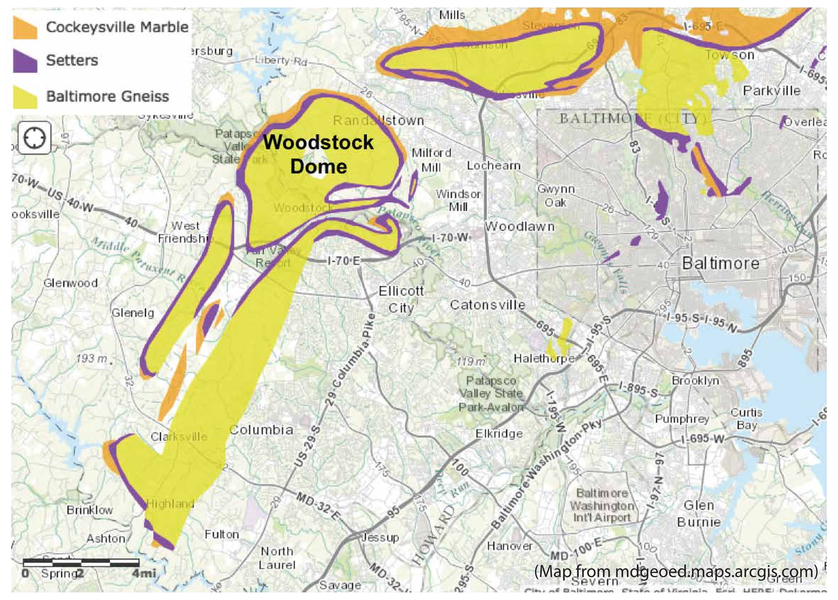

II. Problem & Hypotheses

Petrogenesis of the Setters Formation has not been thoroughly studied and the origin of the tourmaline phase is not well understood.

Chemical analysis of the Setters Formation tourmaline has been used to test the following hypotheses:

1. Tourmaline in the amphibolite-grade metasediments of the Setters Formation exhibits a compositional range along the schorl-dravite solid-solution series, being consistent with previously studied psammites and metapsammites (Henry and Guidotti 1985).

2. Chondrite-normalized REE patterns for tourmaline in the Setters Formation reflects distinct REE patterns associated with metasedimentary host rock.

3. Measurements of boron isotopes in tourmaline from the Setters Formation compared to reference materials to determine the boron to be isotopically heavy associated with a seawater source (δ11B (‰)>0).

III. Major Element Zoning

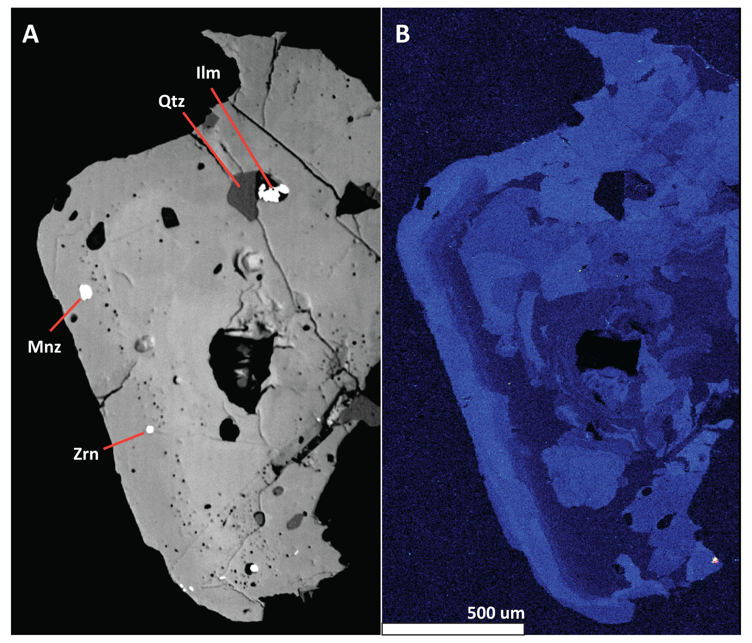

Single tourmaline grain from the Setters Formation displays characteristics of zoning in:

A) BSE image showing distinct rim and core zones. Mineral inclusions include: quartz (Qtz), monazite (Mnz), zircon (Zrn), and illmenite (Ilm).

B) WDS map depicting complex Ca-zoning (Ca content increases from dark to light blue), with a more Ca-rich rim and patchy patterned convolute zoned core.

IV. Tourmaline Speciation

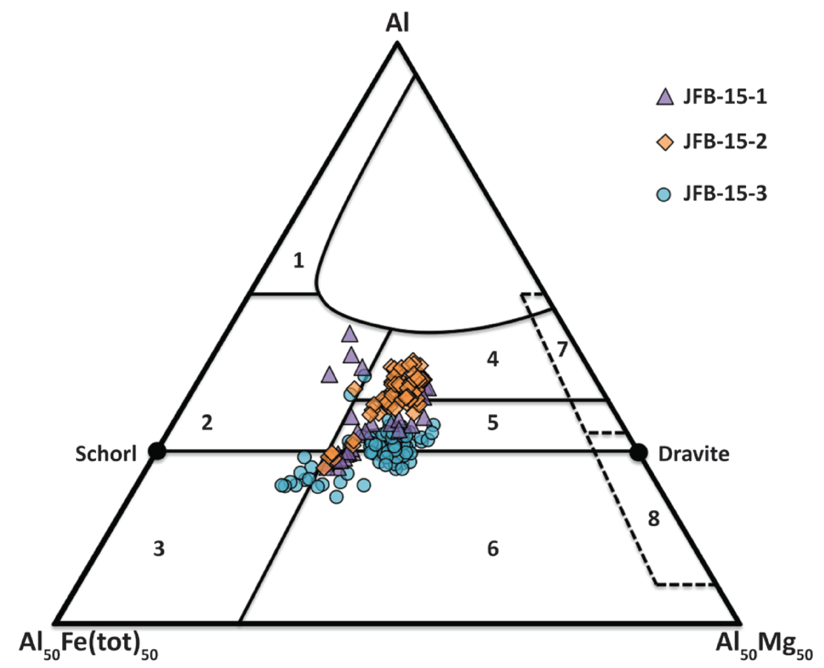

Al-Fe(total)-Mg diagram (molar proportions) for Setters tourmalines plot along the schorl-dravite solid-solution and primarily within zones 4 and 5.

Zone represent 4) metapelites and metapsammites (with Al-saturating phase), 5) metapelites and metapsammites (without Al-saturating phase), as defined by Henry and Guidotti (1985).

V. Total Fe vs Mg

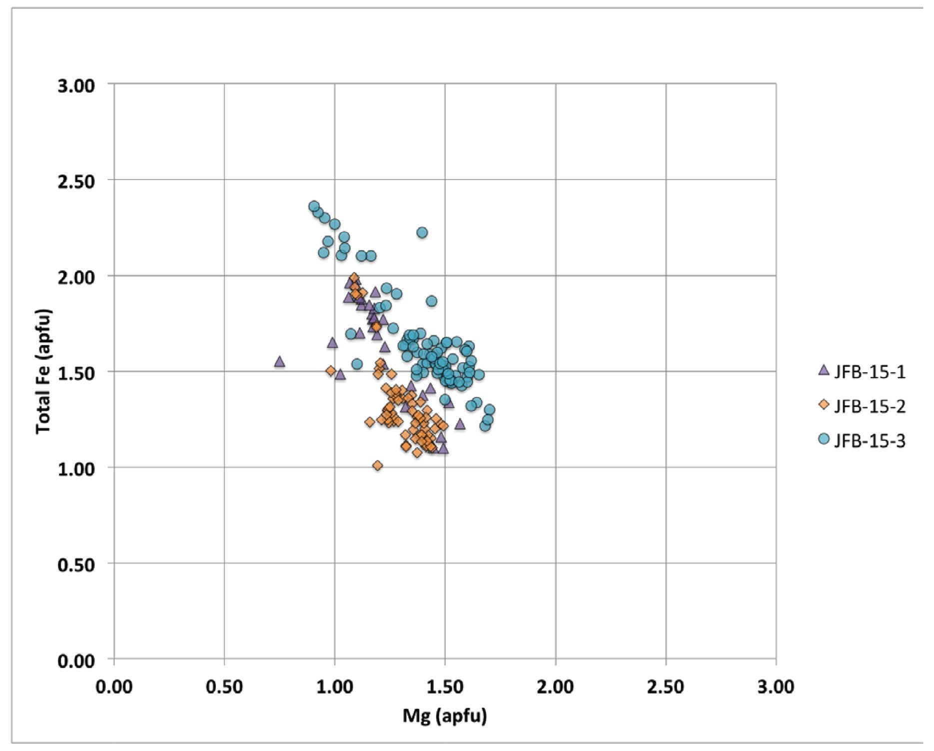

Plot of Fe vs. Mg in tourmaline (plotted based on amount per formula unit, apfu). Fe/Mg ratios for all samples fall in the intermediate range. Distinct compositional variations are represented by the datasets for each location sampled.

VI. Rare Earth & Trace Elements

Plot of the REE trends for Setters tourmaline, with published data from tourmalines in metapelites (Hazarika et al. 2015) and pegmatites (Marks et al. 2013), and seawater (Goldstein & Jacobsen 1988).

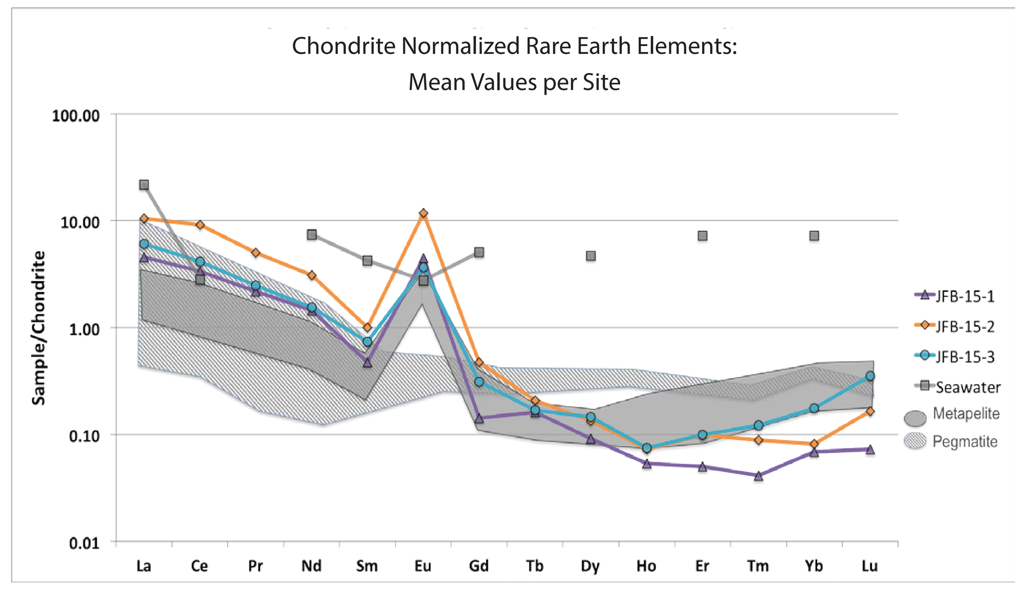

REE (top) and trace element (bottom) data represent the average of all LA-ICP-MS analyses performed for each sample site: 13 spots across 4 tourmaline grains from site JFB-15-1; 68 spots across 14 tourmaline grains from site JFB-15-2; and 35 spots across 15 tourmaline grains from site JFB-15-3.

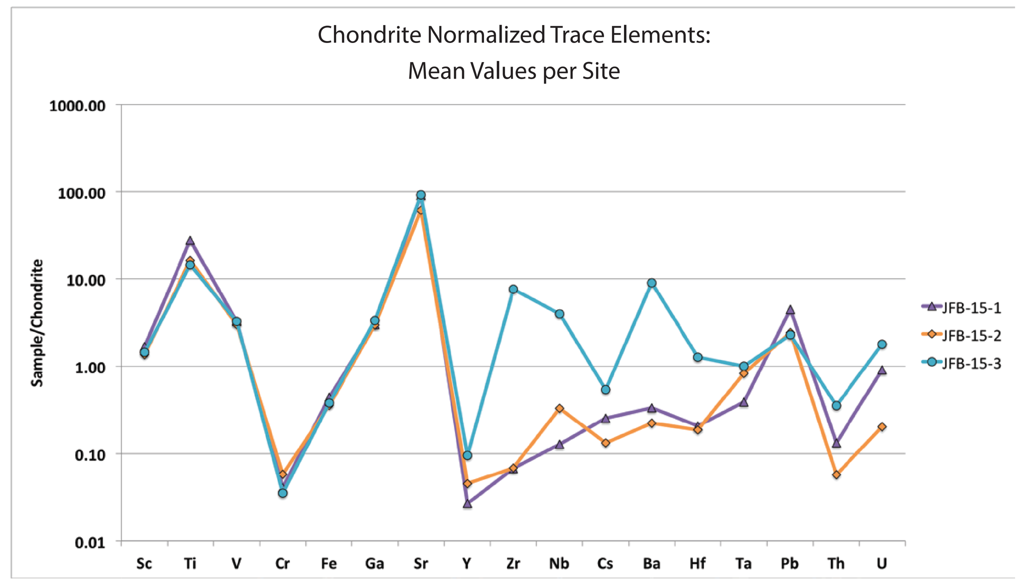

Average trace element trends at all sample sites are similar for the lighter trace elements measured. However, samples from JFB-15-3 display elevated concentrations of the heavier trace elements relative to sites JFB-15-1 and JFB-15-2.

VII. Boron Isotopes

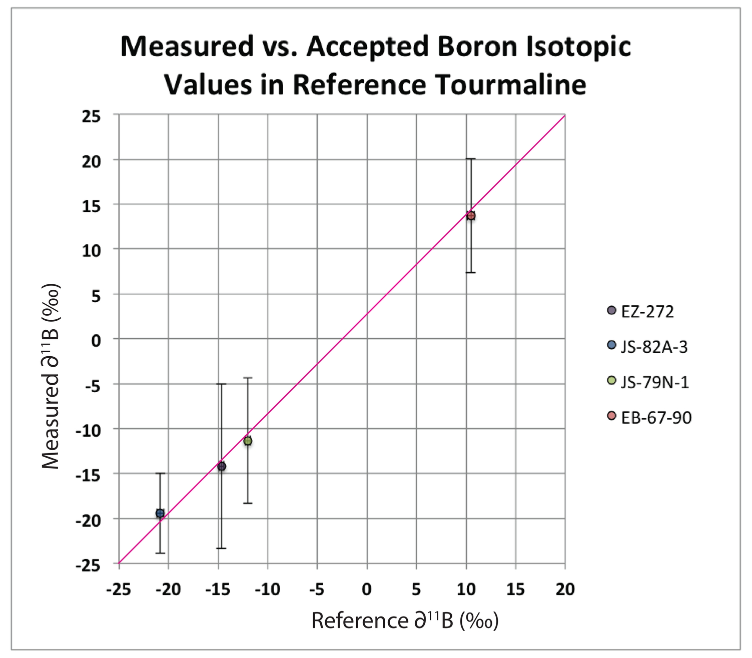

Accuracy of boron isotopic measurements for Setters tourmaline was assessed using natural tourmaline standards. Accepted values for tourmaline standards were determined using TIMS (Palmer & Slack, 1989). LA-ICP-MS measured values for standards are within one standard deviation of a 1:1 trend.

$$\delta^{11}B = \left[\frac{\left(\frac{^{11}B}{^{10}B}\right)_{Sample}}{\left(\frac{^{11}B}{^{10}B}\right)_{SRM\ 951}} - 1\right] \times 1000‰$$

Reference Material	Reference $\delta^{11}B$ (‰)		Measured $\delta^{11}B$ (‰)	
EZ-272	-14.17	±0.23	-14.68	±9.17
EB-67-90	10.47	±0.36	13.72	±6.35
JS-79N-1	-12.00	±0.24	-11.34	±6.97
JS-82A-3	-20.83	±0.37	-19.42	±4.44

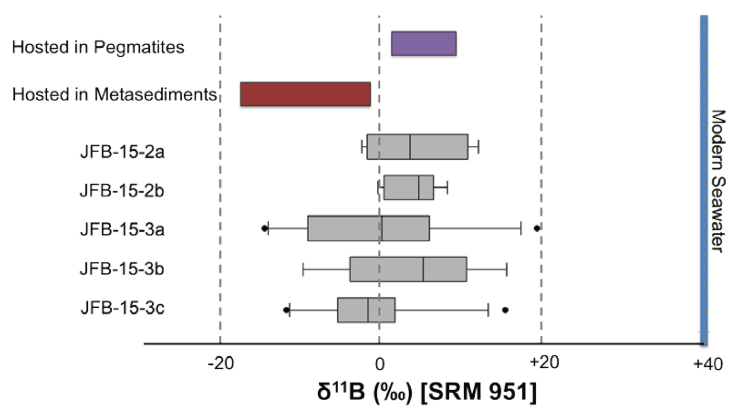

Boron isotope ratio measurements for tourmaline collected in situ using LA-ICP-MS. The blue line indicated the $\partial^{11}B$ value for modern seawater, the purple field indicates the range of $\partial^{11}B$ for tourmaline hosted in pegmatites, and the red field indicates the range of $\partial^{11}B$ for tourmaline hosted in metasediments (from Marschall & Jiang, 2011). Grey fields indicate measurements on Setter tourmaline.

VIII. Discussion

Analysis of Setters tourmaline indicates that distinct compositional variations exist on a local scale. These distinct variations are reflected in the major- and minor-element, and REE data. Correlations between major-element composition and REE abundances appear to be present: JFB-15-2 has the highest Al content and the highest REE abundance of the three sites sampled.

Due to the sampling techniques used, the relationship between compositional variation and schist horizons can not be directly associated. However, there is evidence to indicate that this variation in composition may be present on a sub-meter scale.

IX. Conclusions

Compositional ranges of tourmaline from the Setters Formation are consistent with previously studied pelites and metapelites as determined by EMPA analysis.

Chondrite-normalized REE patterns for tourmaline in the Setters Formation reflects distinct REE patterns associated with metasedimentary host.

A procedure for measuring $\delta^{11}B$ values using LA-ICP-MS was developed during this study. The measurements of boron isotopes in tourmaline from the Setters Formation compared to reference materials determine the boron to be isotopically light ($\delta^{11}B$ (‰)<0) and possibly formed from fluid derived from continental margin sediments and mafic volcanic ash.

References

Fisher, G. (1971). Kyanite-, staurolite-, and garnet-bearing schists in the Setters Formation, Maryland Piedmont. GSA Bulletin , 82, 229-232.
Goldstein, S., & Jacobsen, S. (1988). Rare earth elements in river waters. Earth and Planetary Science Letters , 89, 35-47.
Hazarika, P., Mishra, B., & Pruseth, L. (2015). Diverse tourmaline compositions from orogenic gold deposits in the Hutti-Maski Greenstone Belt, India: Implications for sources of ore-forming fluids. Economic Geology , 110, 337-353.
Hemming, N., & Hanson, G. (1992). Boron isotopic composition and concentration in modern marine carbonates. Geochimica et Cosmochimica Acta , 56, 537-543.
Henry, D., & Guidotti, C. (1985). Tourmaline as a petrogenetic indicator mineral: an example from the staurolite-grade metapelites of NW Maine. American Mineralogist , 70, 1-15.
Marks, M., Marschall, H., Schühle , P., Guth, A., Wenzel, T., Jacob, D., et al. (2013). Trace element systematics of tourmaline in pegmatitic and hydrothermal systems from the Variscan Schwarzwald (Germany): The importance of major element composition, sector zoning, and fluid or melt composition. Chemical Geology , 344, 73-90.
Marschall, H., & Jiang, S. (2011). Tourmaline Isotopes: No element left behind. Elements , 7, 313-319.
Wetherill, G., Tilton, G., Davis, G., Hart, S., & Hopson, C. (1966). Age measurements in the Maryland Piedmont. Journal of Geophysical Research , 71, 2139-2155.